Athenoxat-1, Night Vision Experiments in LEO

Giulio Manzoni, Yesie L. Brama, Meini Zhang
Microspace Rapid Pte Ltd
196 Pandan Loop #06-19, Singapore; +65-97263113
giulio.manzoni@micro-space.org

ABSTRACT

This paper describes the results of the mission of Athenoxat-1, a 3U cubesat developed by Microspace Rapid Pte Ltd of Singapore to demonstrate the functionality of multiple optical payloads in orbit. The Main payload is a night vision imaging system with the maximum aperture allowed by the 3U envelope, while the other four imaging systems use smaller optics for day vision with wide angle and maximum imaging angle. The satellite has been launched in Equatorial LEO by PSLV from India on 16th December 2015 and is healthy operating in orbit since. Imaging experiments are commanded and controlled multiple times per day from Microspace ground station in Singapore. Night imaging of cities, land, sea and celestial subjects as well as day imaging of the Earth surface for environmental and meteorological purposes has been successfully demonstrated. In addition to the imaging functionality, the cameras have been used to complement the Attitude Determination by detecting the Earth horizon.

INTRODUCTION

More and more nanosatellites have been launched or are being manufactured for various applications, such as remote sensing, vessel/flight radio tracking, environmental studies, and new technology demonstrations. Microspace Rapid Pte Ltd has also previously launched a nanosatellite, POPSAT-HIP1, which has successfully demonstrated attitude maneuver with cold gas micropropulsion (1). The next mission of Microspace was to demonstrate night imaging on a cubesat, Athenoxat-1. Night imaging mission on cubesats is not yet common and perhaps was attempted only by very few cubesats, if not only by AC-4 (2). Athenoxat-1 aimed to demonstrate the highest practical resolution achievable within the project constrains and the results obtained show the accomplishment of the mission.

SATTELITE AND PAYLOADS

Athenoxat-1, presented in Figure 1, is a 3U cubesat with high efficiency body mounted solar panels, 4 deployable double faced solar panels developed in house, and high battery capacity to supply up to 20W in eclipse to all subsystems. It comprises the standard cubesat subsystems such as OBC and EPS, and it uses a half-duplex UHF radio for telecommands and data downlink on a dipole antenna. It is currently orbiting at equatorial orbit of 15° inclination at ~550km altitude.

The main payload of the satellite is a night vision optical payload designed to have 25m resolution, using a fast optics designed and developed by Microspace which occupies 1.2U and is equipped with a CCD imaging sensor. The secondary payloads are four imaging systems for day vision as well as auxiliary attitude determination sensor for detecting the Earth horizon, and reaction wheels made in-house for the attitude control system.

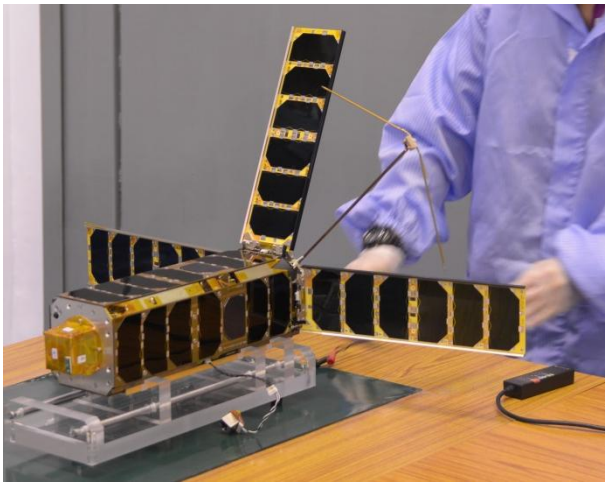

Figure 1: Athenoxat-1 at the ISRO –Sriharikota integration facility

All optical payloads can snap simultaneous images, which is a very useful feature for pointing comparison and identification studies as well as for supporting the attitude control. Figure 2 shows 4 images snapped on Nadir pointing over central Africa including also a night vision image from the main payload for size comparison. Features from lake Albert and lake Victoria are evident in the Nadir pointing fish-eye and wide angle image. It can be noticed how the slight eccentricity of the Nadir pointing fish-eye is matched by the slightly different extension of the side fish-eye images.

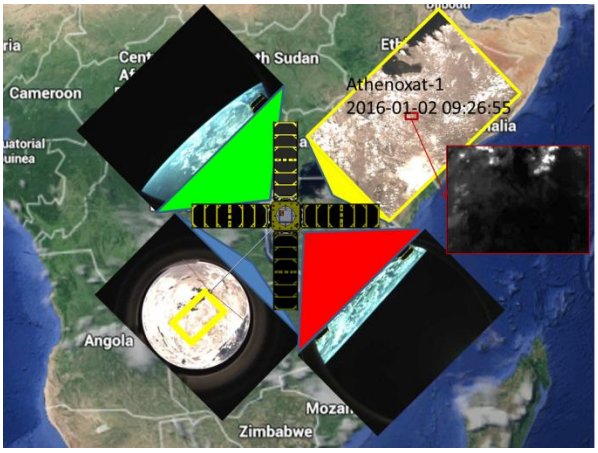

Figure 2: Simultaneous day images and night image

ATTITUDE DETERMINATION AND CONTROL

The ADCS is based on the classic use of Magnetometer, Sun sensors and Gyroscopes for determination, and Magnetorquers and Reaction Wheels for control of the satellite attitude. For two axes (X,Y) the magnetorquers are embedded in the body mounted solar panels while for the third axis (Z) the magnetorquer is an air coil made in-house. The reaction wheels are also built in-house and they allow a complete re-orientation of the satellite in about 60sec. The attitude determination algorithms developed for Athenoxat have also demonstrated the capability to obtain the Nadir vector from the fisheye images of the Earth by recognizing the Earth Horizon, correcting the fisheye distortion, and calculating the position of the Earth center from the circle fitting of the detected horizon points. Star tracker and GPS receiver have not been considered for this mission due to restrictions of power, mass, volume and project budget.

RESULTS AND DISCUSSIONS

In this section, the results and discussions about the wide angle imaging, fisheye imaging, and the main payload imaging are presented.

(i) WIDE ANGLE IMAGING

a. Resolution

The resolution of the wide angle camera can be estimated from some details of the images. As shown in Figure 3 and Figure 4, details with size around 250~450m on the Earth can be discerned clearly.

By comparing the smallest features that can be distinguished with Google map, it is safe to estimate a resolution of about 300m for the wide angle imaging system.

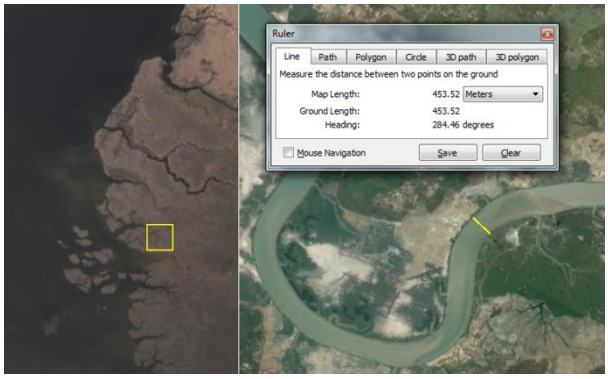

Figure 3: Guinea Bissau, detail of Rio Geba

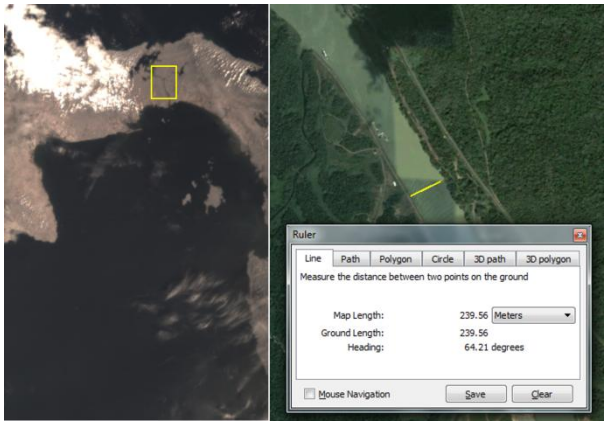

Figure 4: Panama Canal

In the image of Singapore shown in Figure 5, based on the visible Bedok reservoir (about 1km wide) and other relevant features such as the separation between Sentosa Island and Singapore, Pandan and MacRitchie Reservoirs, Ubin Island, etc., the 300m resolution can be demonstrated as well.

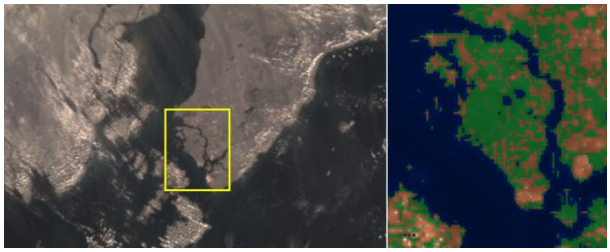

Figure 5: Image of Singapore in original and artificial colors based on RGB values

It is also interesting to appreciate the capability to identify Changi Airport airstrips with the bare land on its side and similar bare land in nearby Malaysia. The artificial color is given according to the RGB values of each pixel. Even though the sensor is not specifically for remote-sensing purpose, the combination of RGB channels behaves differently for vegetation, sea, cloud,

and bare land area, which makes it possible to give different color artificially to tell various features apart.

b. Quasi real-time scouting

Large Earth Observation (EO) satellites with high resolution imaging payloads are very expensive to purchase, launch and operate and it is very important to make the best use of their passes over the areas to be observed. This requires a preliminary knowledge of the weather conditions, to avoid spending the expensive imaging time on cloudy areas. Unfortunately it is not always possible to rely on weather forecasts and nowcast especially if remote areas of foreign countries need to be imaged.

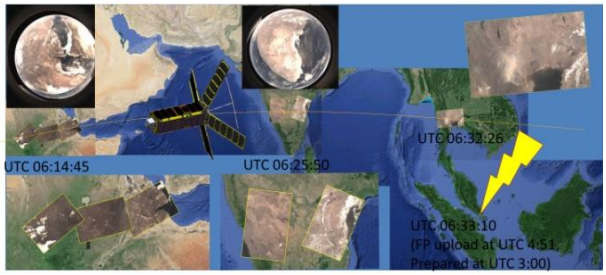

Figure 6: Quasi real-time scouting activity of Athenoxat-1

Athenoxat-1, with its multiple imaging payloads, can find very good use if present in a leading formation flight position to complement the known weather information so that other large EO trailing satellites can be aided during their following passes to aim at the areas of interest free of clouds.

Such activity has been fulfilled successfully by Athenoxat-1. An interesting sequence of 6 images were taken from the Red Sea to India and Thailand and downloaded immediately available on the coming pass over Singapore with a maximum delay of just 20 min from the first snap and 1min from the last one as shown in Figure 6.

This exercise fully validates the use of Athenoxat-1 as "scouting nanosatellite" for tactical imaging, weather nowcast, environmental warning and in general to complement other imaging systems with its wide angle view of large regions (1000km or more) with sub-km resolution.

c. Weather and haze imaging

Another interesting application of the Wide Angle Camera is for the observation of the Haze Plumes produced by the forest fires in Indonesia and Malaysia. A comparison between pictures taken by Athenoxat-1 and the Japanese geostationary satellite Himawari-8/9, which was supplied by the P-Tree System – Japan Aerospace Exploration Agency (JAXA) (3) is presented in Figure 7.

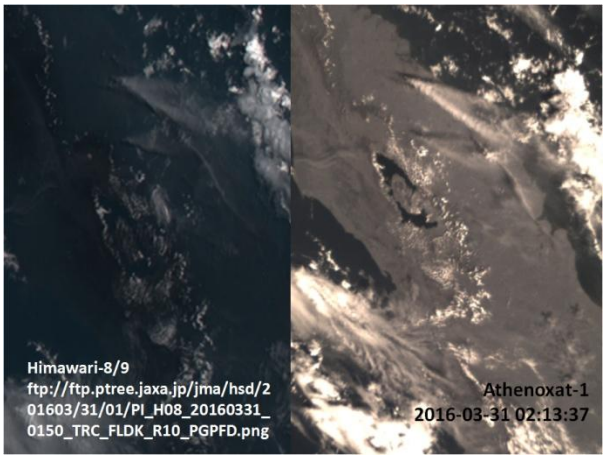

Figure 7: Haze Plume picture comparison between Himawari-8 and Athenoxat-1

The texturing of the haze plume is much more evident in the Athenoxat-1 picture which is taken on Nadir pointing versus the Himawari-8/9 picture that is originally slanted from the GEO position and requires heavy orthorectification. Resolution estimated for the Athenoxat-1 image is below 500m while Himawari-8/9 is declared as 0.5 – 1km (4).

It can also be noted that the Athenoxat-1 image does not require large orthorectification since it has already been almost Nadir Pointing hence it shall have a minimal distortion and loss of information when compared to Himawari-8/9 which, except for its central viewing region is located at a very different Longitude than its largest viewing areas.

(ii) FISH EYE IMAGING AND NADIR DETERMINATION

To complement the Attitude Determination, Nadir vector acquisition has been added in the satellite by means of Earth horizon detection. It is achieved by having three fisheye cameras mounted on front and side faces of satellite body facing different directions to detect the Earth horizon, from which the nadir vector can be derived. This solution works properly when the Earth is well illuminated. In Figure 8, the detection of Earth horizon points and the derived nadir vector are shown. The red points are detected edge points of the earth in fisheye image, while the green points are corrected points for removing fisheye distortion (4). Based on circle fitting of the corrected points, the actual Earth is plotted in green curve. Subsequently, the nadir vector is pointing from the satellite to the center of the

Earth, which is marked as a blue point in the figure. The nadir vector calculated by the algorithm is [-0.1069, 0.0724, 0.9916] for X-, Y- and Z-axis of the satellite body frame, respectively. Comparing with the actual image shown in Figure 8, it is obvious to see that the nadir vector is almost accurate. In addition, the algorithm is also robust to reject outliers from all the detected edge points which may come from sunshine or reflections. It can be seen in Figure 9.

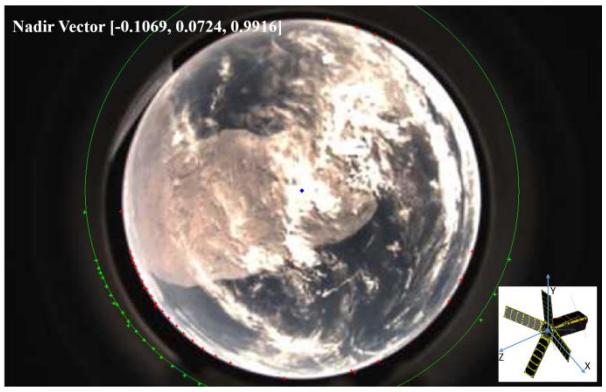

Figure 8: Detection of Earth horizon points and the derived nadir vector

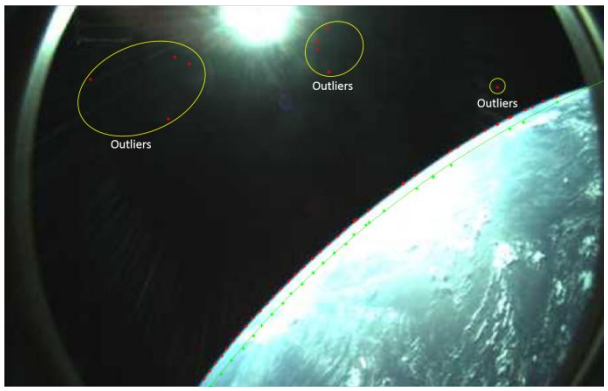

Figure 9: The algorithm is robust to reject outliers among all the detected edge points

The limitation of this solution, with the sensors presently used, is that when the views are not bright and clear enough, the recognition will be degraded and thus may give incorrect nadir vector.

(iii) MAIN PAYLOAD IMAGING

Night vision has been successfully demonstrated on multiple subjects and 25m ground sampling distance (GSD) has been achieved as expected for the selected optical configuration and available sensor. Coverage is about 21km diagonal on Nadir imaging.

a. Resolution

As shown in Figure 10, it is the Olongapo harbor, The Philippines captured by the main payload. The features recognized in the image allow the resolution assessment of the imaging system.

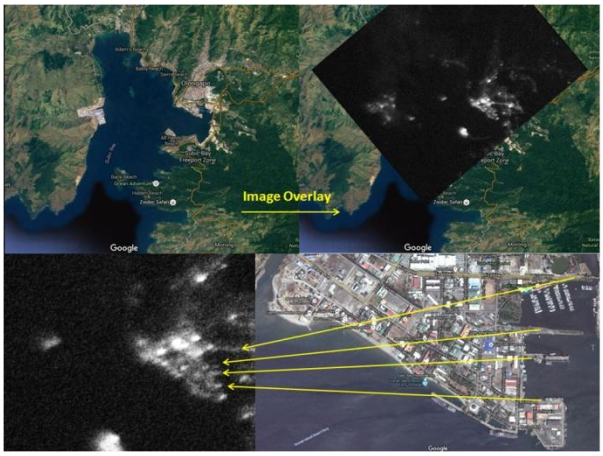

Figure 10: Olongapo harbour (near Manila)

At least 4 distinct features are very easily recognized in the image: Rizal Hwy, Subic Bay Freeport Zone with piers and international airport, Hanjin Shipyard (opposed in the bay). Also some ships appear in the middle of the harbour.

A more detailed analysis of the picture can be done by comparing the size of the piers to their image as done in Figure 10 as follows:

- Rizal Hwy bridge: 50m
- Land protrusion at Causeway Road: less than 50m
- Pier at Quezon Street: 25m
- Subic dock: 100 to 200m

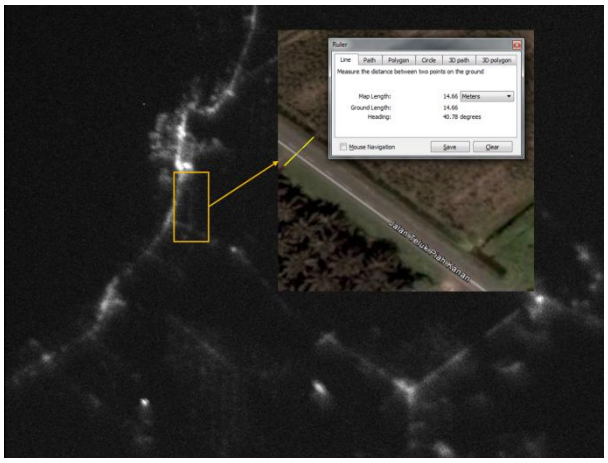

Figure 11: Kuala Selangor, Malaysia

Another example to demonstrate the resolution is an image captured for Kuala Selangor, Malaysia, shown in

Figure 11. The road as narrow as 15m is still able to be discerned. It confirms that the resolution of 25m can be achieved definitely and probably even better.

b. Pointing accuracy

The pointing accuracy can be demonstrated from Stars and Moon imaging.

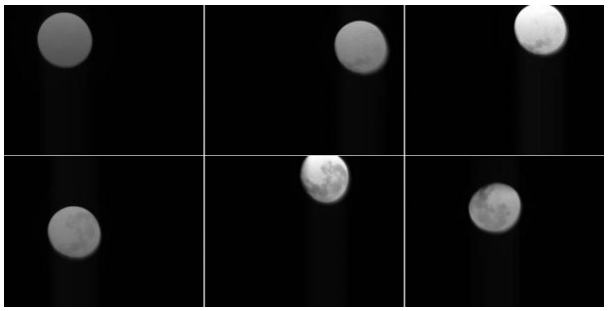

Figure 12: Various attempts to image the Moon

The captured images of Moon are displayed in Figure 12. From the various successful pictures it can be appreciated that the pointing accuracy is within the range of 0.5° evaluated by observing that the moon itself (0.5° apparent size) is almost tangent to the center of the image.

The Carina Nebula was also captured and identified, as shown in Figure 13. All the images were taken in the experiment of pointing at the center of Carina Nebula. Since all the stars are identified, it is easy to assess the pointing accuracy by comparing the center of each image with the theoretical pointing center. The average pointing accuracy is ~0.9° in this experiment.

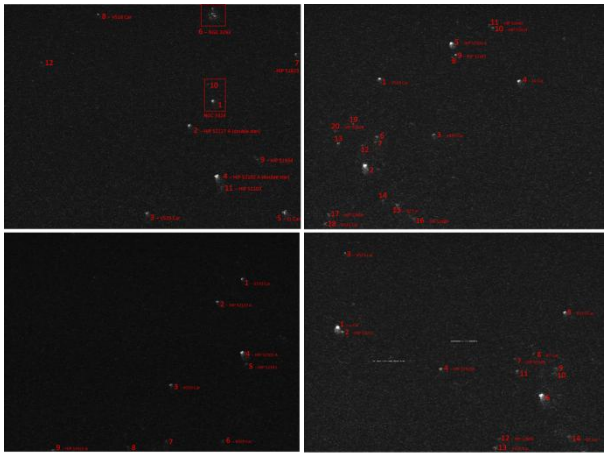

Figure 13: Identified images of Carina Nebula

c. Pointing stability

Stability of the platform can be observed by analyzing the distribution of a stretch of images taken in the same inertial pointing experiment. For example, the estimation can be done for a series of images taken for the city of Singapore and Johor Bahru, shown in Figure 14. The subgraph plots the linear fitting of the actual image positions. By measuring the deviation from the actual image positions (shown as blue dots in the subgraph) with the ideal distribution positions (represented as green line in the subgraph); in this case the stability is estimated to be within 3σ = ~0.27°.

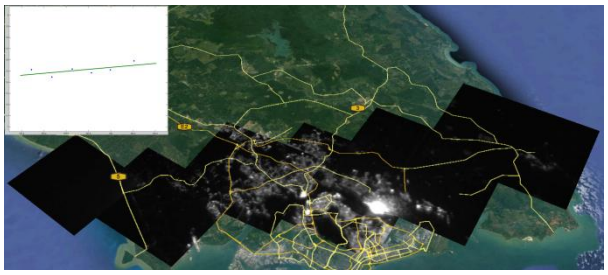

Figure 14: Stretch of images of City Singapore and Johor Bahru

CONCLUSION

Athenoxat-1 has been developed very quickly in only 1 and half year after the launch of POPSAT-HIP1 thanks to the adoption of the same basic satellite bus. In such way Microspace has refined its reliable 3U cubesat bus capable of hosting payloads as big as 2Us.

Athenoxat-1 has demonstrated a very efficient set of imaging capabilities in just one Cubesat nanosatellite. The day images can be used to study the hydrology and agriculture of lands, the distribution of clouds in real time, origin and development of haze plumes and many other environmental studies.

The high resolution night images, for the first time available on a nanosatellite, can be used for study of urbanization, traffic and tracking at night as well as for fires detection and monitoring. Athenoxat has the top performance in the field of nanosatellites night vision with GSD as good as 25m and a pointing accuracy within 1°.

Several attitude control modes are available and presently under experimental characterization so that algorithms and hardware can be further improved in the next versions of Microspace nanosatellites based on the lessons learnt with POPSAT-HIP1 and Athenoxat-1.

ACKNOWLEDGMENT

The authors wish to acknowledge the colleagues James Lim, Ankur Gupta and Naushad Rahman for the coding used in the satellite control and ground station data analysis. Furthermore, the company Gomspace Aps is acknowledged for supplying the main COTS subsystems of Athenoxat-1, and ISIS BV for supplying the ISIPOD for the satellite deployment. Athenoxat-1 has been launched by PSLV on a slot arranged by NTU. Google Map and Google Earth have been used throughout the project for geographical reference.

REFERENCES

1. *Cubesat Micropropulsion Characterization in Low Earth Orbit.* **Manzoni, Giulio and Brama, Yesie L.** Logan : Utah State University, 2015. 29th Annual AIAA/USU Conference on Small Satellites.

2. **The Aerospace Corporation.** Research: Small Satellites - Leading the Development of Small Spacecraft Technology. [Online] [Cited: July 5, 2016.] http://www.aerospace.org/research/fundamental-research-and-development/randdspace-materialssmall-sats/.

3. **Japan Aerospace Exploration Agency, Earth Observation Research Center.** JAXA Himawari Monitor. [Online] [Cited: April 5, 2016.] ftp://ftp.ptree.jaxa.jp/jma/hsd/201603/31/01/PI_H08_20160331_0150_TRC_FLDK_R10_PGPFD.png

4. **Japan Meteorological Agency (JMA).** Imager (AHI). *JMA/MSC: Himawari-8/9 Imager (AHI).* [Online] [Cited: April 5, 2016.] http://www.data.jma.go.jp/mscweb/en/himawari89/space_segment/spsg_ahi.html.

5. *A generic non-linear method for fisheye correction.* **Dhane, Pranali, Kutty, Krishnan and Bangadkar, Sachin.** 10, s.l. : International Journal of Computer Applications (0975-8887), August 2012, Vol. 51.